

# Reduction of Alternating-Current Losses in (RE)Ba<sub>2</sub>Cu<sub>3</sub>O<sub>x</sub> Monolayer and Double-Layer Superconducting Power Cables

H. Noji

Department of Electrical and Computer Engineering, National Institute of Technology, Miyakonojo College  
473-1 Yoshio-chou, Miyakonojo City, Miyazaki Prefecture 885-8567, Japan  
noji@cc.miyakonojo-nct.ac.jp

**Abstract**-The purpose of this research was to obtain new methods for decreasing alternating-current (AC) losses when transport currents pass through high critical-temperature superconducting power cables. The cables used in this study were composed of (RE)Ba<sub>2</sub>Cu<sub>3</sub>O<sub>x</sub> (REBCO) superconducting tapes. The AC losses in monolayer and double-layer REBCO cables were calculated by a two-dimensional finite-element method (2D FEM). The cable parameters were those specified for the REBCO cables manufactured by Furukawa Electric Co. Ltd. In the monolayer cable, the loss in one tape of the cable was drastically decreased by increasing the tape number  $N$  from 25 to 100 (maintaining a constant critical current  $I_C$  of 1,140 A in the cables). The loss in the monolayer cable also decreased as the tape width  $w$  decreased from 4 mm to 1 mm. When calculating the loss in the double-layer cable,  $N$  in the first and second layers ( $N_1$  and  $N_2$ , respectively) were the same as  $N_1 = N_2 = 16$ , and the layer currents were assumed equal. It was observed that the loss drastically decreased as the relative tape-position angle between the layers increased, becoming minimized at a relative angle of 0.5. This reduction was caused by the cancelation of the vertical field between the first and second layers. At this relative angle, the opposite edges of the tapes in the two layers were minimally separated, and the vertical fields were cancelled out.

**Keywords**- High- $T_C$  Superconductor; Superconducting Power Cable; REBCO Tape; AC Loss; Finite-Element Method

## I. INTRODUCTION

Superconducting power cables are used in actual lines, because they can provide high power transmission with low current loss. Electrical components of cables are constructed from (BiPb)<sub>2</sub>Ba<sub>2</sub>Cu<sub>3</sub>O<sub>x</sub> (BSCCO) or (RE)Ba<sub>2</sub>Cu<sub>3</sub>O<sub>x</sub> (REBCO) superconducting tapes. REBCO tapes have been extensively researched worldwide because they provide high critical current density  $J_C$  with low current losses [1, 2]. Low current loss rates are necessary for practical cable applications because the costs of liquid nitrogen cooler are reduced. Reduction of the losses in REBCO cables has been attempted in many studies [3–5]. Mukoyama, et al. fabricated a REBCO cable with two layers and successfully reduced the loss by adjusting the helical pitch of the tapes in each layer until the layer currents were equalized [6]. The author calculated the loss in Mukoyama's cable using an electric circuit model and verified the strong agreement between the model results and the results of a previous experiment [7]. In this research, the loss in each REBCO tape was calculated by the thin-strip Norris equation. However, the Norris equation determines the loss in a single isolated tape, which differs from that of a tape connected to a cable. Therefore, an analytical model for cable loss was constructed using the two-dimensional finite-element method (2D FEM). FEM analysis is a practical and commonly used method for calculating losses in REBCO cables. Amemiya, et al. reported a numerical model [8] and methods for computing reduced AC losses [9]; however, their model was complicated and assumed the thin-strip approximation (1D model) of the superconductor layer of the REBCO tape. Previously, the author developed a new electric-circuit model that calculated the layer currents in REBCO cables [10]. The current losses in REBCO cables can be calculated by combining the electric circuit model with 2D FEM. In this combination, the loss calculation becomes a quasi-3D electromagnetic field analysis. Therefore, 2D FEM codes were constructed and their reliability was confirmed. This numerical model (described in the next section) was simpler than Amemiya's model. Moreover, different from Amemiya, et al., the author used a normal 2D model of the superconductor layer of the REBCO tape. By the application of the 2D FEM codes, a new method for decreasing losses in REBCO cables was found, which will be described later. The 2D FEM was programmed in the commercial software COMSOL.

## II. CALCULATIONS

The basic equations of the 2D FEM are described below, assuming that the cross-section of the tape lies in the  $x$ - $y$  plane and that the current flows parallel to the  $z$ -axis. The current density  $J_z$  can then be determined by Ampere's Law, as in the following:

$$J_z = \frac{dH_y}{dx} - \frac{dH_x}{dy}, \quad (1)$$

where  $H_x$  and  $H_y$  are the magnetic fields along the  $x$ - and  $y$ -axes, respectively. The electric field  $E_z(J_z)$  can then be determined by Faraday's Law, as in the following:

$$\begin{bmatrix} \mu_0 & 0 \\ 0 & \mu_0 \end{bmatrix} \cdot \begin{bmatrix} \frac{dH_x}{dt} \\ \frac{dH_y}{dt} \end{bmatrix} + \nabla \cdot \begin{bmatrix} 0 & E_z(J_z) \\ -E_z(J_z) & 0 \end{bmatrix} = \begin{bmatrix} 0 \\ 0 \end{bmatrix}, \quad (2)$$

where  $E_z(J_z)$  is the current-dependent electric field, and  $\mu_0$  is the magnetic permeability in a vacuum. The model calculates this field by the following empirical formula:

$$E_z(J_z) = E_0 \left( \frac{J_z}{J_C} \right)^\alpha, \quad (3)$$

where  $E_0$  and  $\alpha$  are constants set to  $E_0 = 1 \times 10^{-4}$  V/m and  $\alpha = 25$ .  $E_0$  is a criterion field for measuring the critical current  $I_C$  in the voltage–current ( $V$ – $I$ ) property of a superconductor, and  $\alpha$  determines the properties of a REBCO superconductor. In Mukoyama's cable, the critical current  $I_C$  in one tape of the double-layer cable was calculated to be  $I_C = 45.6$  A, the tape width  $w$  was 4 mm, and the thickness  $d$  of the superconductor in the tape was 1  $\mu$ m. From these specifications, the critical current density  $J_C$  was calculated to be  $1.14 \times 10^{10}$  A/m<sup>2</sup>. The AC loss  $Q$  can be obtained by the following:

$$Q = f \cdot \int_{\frac{1}{f}} dt \int_S E_z(J_z) \cdot J_z dS, \quad (4)$$

where  $f$  is the frequency (here,  $f = 50$  Hz).

In the monolayer cable calculations,  $d$  was fixed at 1  $\mu$ m and  $w$  was varied from 1 mm to 4 mm. In the calculations of the double-layer cable,  $w$  was fixed at 4 mm. To maintain the same  $J_C$  in the monolayer cable, the  $I_C$  was set to 45.6 A for  $w = 4$  mm, 22.8 A for  $w = 2$  mm, and 11.4 A for  $w = 1$  mm. The specifications of the double-layer cable were the same as those of Mukoyama's cable [7] and are listed in Table 1. Figure 1 illustrates a cross-section of the double-layer cable. The specifications of the monolayer cable are the same as those of the first layer in the double-layer cable.

TABLE 1 SPECIFICATIONS OF DOUBLE-LAYER CABLE

<b>Tape width <math>w</math></b>	4 mm
<b>Tape thickness</b>	0.1 mm
<b>Thickness of superconductor <math>d</math></b>	1 $\mu$ m
<b>Outer radius of former <math>r_f</math></b>	16 mm
<b>Inner radius of first layer's superconductor <math>r_1</math></b>	16.099 mm
<b>Inner radius of second layer <math>r_s</math></b>	16.25 mm
<b>Inner radius of second layer's superconductor <math>r_2</math></b>	16.349 mm
<b>Number of tapes in first layer <math>N_1</math></b>	4 – 25
<b>Number of tapes in second layer <math>N_2 (= N_1)</math></b>	4 – 25
<b>Critical current of the tape <math>I_C</math></b>	45.6 A

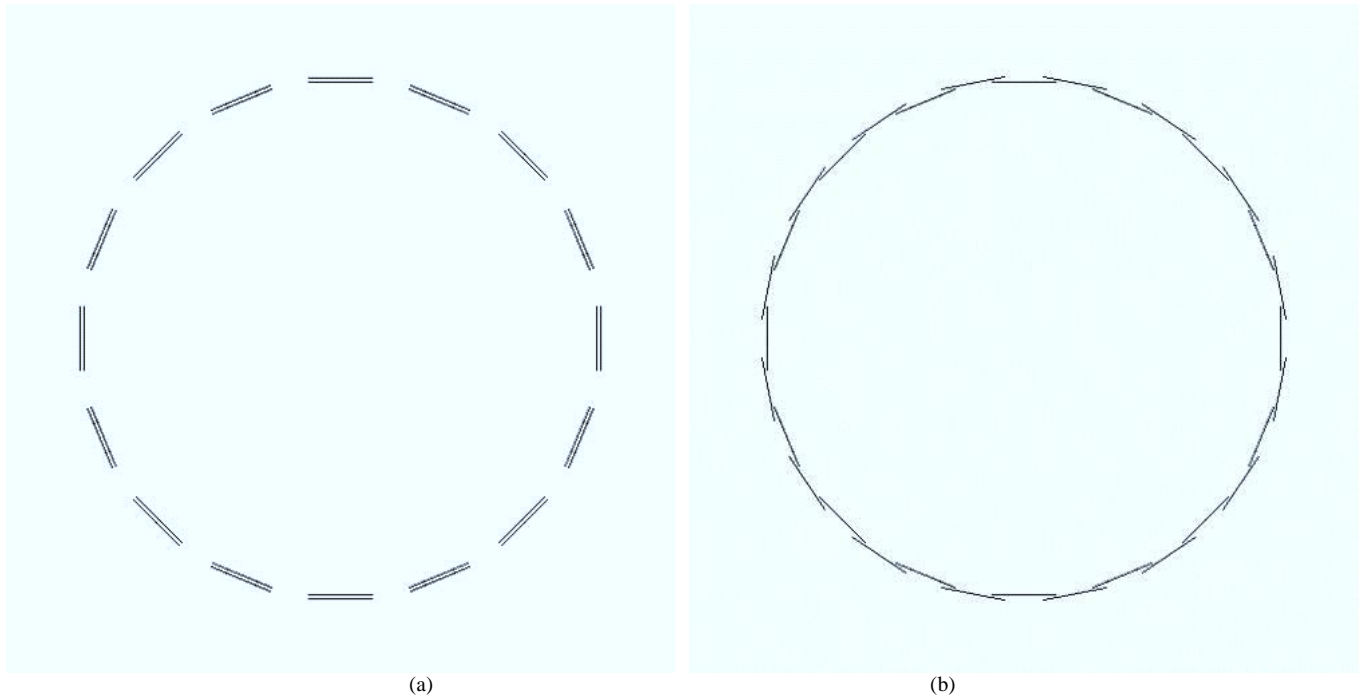


Fig. 1 Cross-sections of double-layer cable with (a)  $\theta/\theta' = 0$ ; and (b)  $\theta/\theta' = 0.5$

### III. RESULTS AND DISCUSSION

#### A. AC Loss in Monolayer Cable

Monolayer cables are composed of several REBCO tapes. The radius of the cable and the width of the tape were fixed at  $r_f = 16$  mm and  $w = 4$  mm, respectively. The former is the cable core around which the REBCO tapes are wound. In a three-phase superconducting cable, the cable core consists of corrugated SUS pipe. Liquid nitrogen is passed through this pipe to cool the placed straight along its length direction. First, the AC losses in the monolayer cables were calculated. Figure 2 plots the normalized AC losses  $Q/N$  in the monolayer cables versus the current ratio  $I_a/I_C$  as  $N$  increased from 4 to 25 (25 is the largest tape number that can be used to construct a monolayer cable with the specified radius). The normalized AC loss  $Q/N$ , obtained by dividing the cable loss by the tape number, gives the loss in a single tape. At the current ratio,  $I_a/I_C$ ,  $I_a$  and  $I_C$  denote the peak transport current and the critical current of the monolayer cable, respectively. To obtain the  $I_C$  of the monolayer cable, the  $I_C$  of the tape (45.6 A) was multiplied by  $N$ . The dashed lines in Fig. 2 are guides for the eye. The loss  $Q_{NS}$  calculated by the Norris equation for a thin strip is indicated by the red bold line in this figure. The Norris equation is given by the following:

$$Q_{NS} = \frac{I_C^2 \mu_0 f}{\pi} \{ (1 - i) \ln(1 - i) + (1 + i) \ln(1 + i) - i^2 \}, \quad (5)$$

where  $i$  is the normalized transport current,  $i = I_a/I_C$ . When  $N \leq 8$ ,  $Q/N$  is almost equal to  $Q_{NS}$ , for the following reason. When only a few tapes comprise a monolayer cable, the field applied to each tape is almost entirely self-contained and the magnetization loss is almost zero because the gap between adjacent tapes is sufficiently wide. Under these circumstances,  $Q/N$  can be approximated by the Norris equation. When  $N \geq 16$ ,  $Q/N$  decreases with increasing  $N$  and is minimized at the maximum tape number  $N = 25$ . At  $N = 25$ ,  $Q/N$  is two orders of magnitude lower than  $Q_{NS}$  at a low normalized current ( $I_a/I_C = 0.4$ ) and is one order of magnitude lower at a high normalized current ( $I_a/I_C = 1$ ). The decreased losses as  $N$  increases from 16 may be explained by the vertical magnetic field generated at the edge of the tape when current passes through the tape in the cable. The vertical field increases the loss but is cancelled by the inverse vertical field generated in the gaps between the adjacent tapes. Increasing the tape number decreases the gaps and enhances the cancelation of the vertical field. The decreased loss as  $N$  increases is called the gap effect [8]. In fact, the amount by which the gaps reduce may be calculated by applying the following [11]:

$$g = \frac{2\pi r_1}{N} - w \quad (6)$$

for various  $N$ . The normalized AC losses  $Q/N$  in the monolayer cables were plotted as functions of the gap  $g$  for various normalized currents  $I_a/I_C$ , as shown in Fig. 3. As can be seen, the normalized losses were drastically decreased when  $g \leq 1$  mm, and the decreasing slope steepened with decreasing normalized currents. These results showed that reducing the gaps between tapes effectively reduced the losses in the cable, as was also reported in Ref. [12].

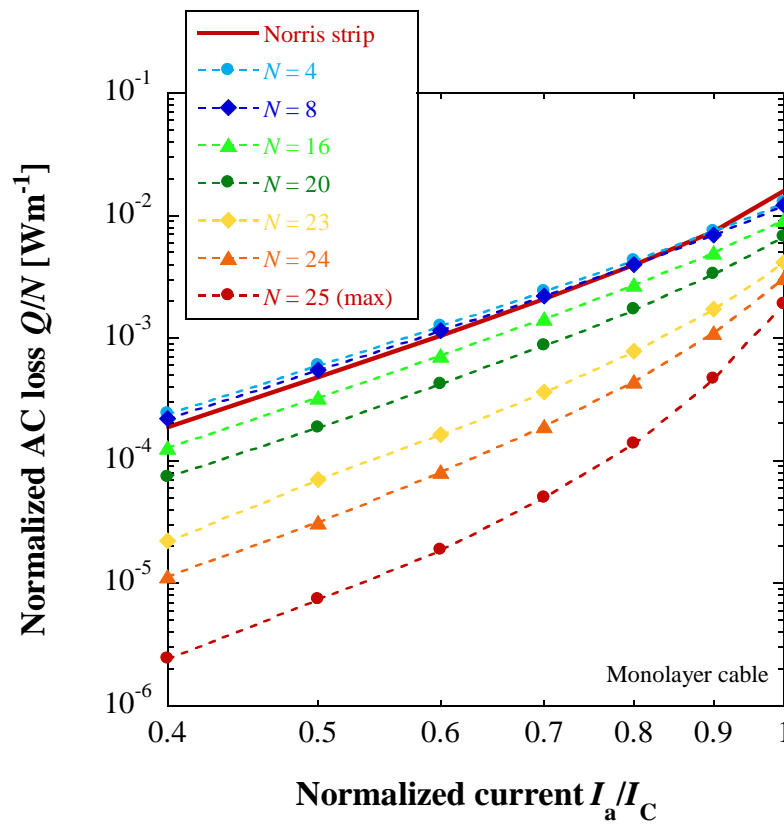


Fig. 2 AC losses in monolayer cables versus transport current for different tape number  $N$

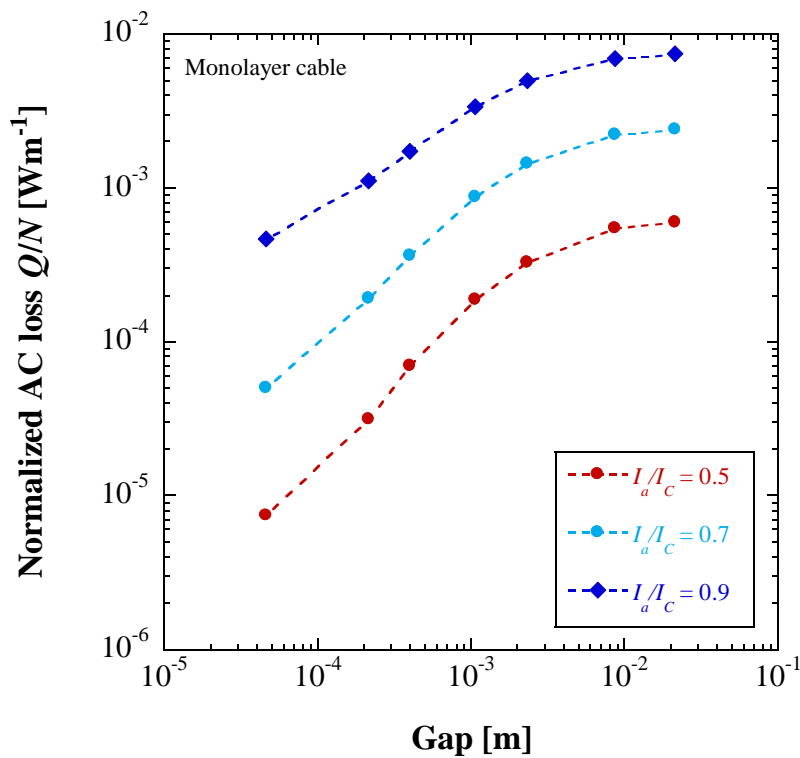


Fig. 3 AC losses in monolayer cable versus gap between tapes, determined at different transport currents (normalized by critical current)

Given that the radius of the cable and the tape width were fixed at  $r_1 = 16$  mm and  $w = 4$  mm, respectively, the gap  $g$  was minimized at  $g = 21.24$   $\mu\text{m}$  when the tape number was maximized at  $N = 25$ . To further decrease the gap,  $w$  was reduced to one-half and one-quarter of its original value and the corresponding tape numbers were increased to 50 and 100, respectively,

to fix the  $I_C$  of the cable at 1459 A. At  $w = 2$  mm and 1 mm,  $g$  was decreased to  $10.62 \mu\text{m}$  and  $5.31 \mu\text{m}$  when  $w$  was reduced to one-half and one-quarter of its original value, respectively. Figure 4 plots the AC losses  $Q$  versus the normalized current  $I_a/I_C$  for the three tape widths  $w$ . In this figure, the bold red line shows the result of the Monoblock model [13], calculated as the following:

$$Q_M = \frac{I_m^2 \mu_0 f}{\pi} \left\{ i' - \frac{i'^2}{2} + (1 - i') \ln(1 - i') \right\}, \quad (7)$$

where

$$i' = \frac{I_a}{I_m} \quad (8)$$

and

$$I_m = \frac{r_o^2 I_C}{r_o^2 - r_i^2}, \quad (9)$$

where  $r_o$  and  $r_i$  denote the outer and inner radii of the monolayer cable, respectively. Here,  $r_o = 16.099$  mm and  $r_i = 16.1$  mm. This model computed the losses in hollow cylindrical superconductors. As is evident in Fig. 4, the losses were reduced as the tape width decreased, most likely due to the gap effect. However, the gap effect seemed to only hold over a limited range. For example, when  $w = 1$  mm and  $N = 100$ , the losses approached the results of the monoblock model as the normalized current decreased. As mentioned above, decreasing the gap encourages cancelation of the vertical magnetic fields. In contrast, the monoblock model is not designed for vertical field configurations, because it assumes that the magnetic field in a hollow cylindrical superconductor is generated in the circumferential direction. The author also calculated the loss for a hollow cylindrical superconductor with a thickness of  $1 \mu\text{m}$  by 2D FEM analysis. In Fig. 4, the blue squares illustrate the losses of this superconductor. The losses were much lower than those calculated by the monoblock model. Therefore, the cylinder-calculated losses probably represented the minimum limit for the monolayer cable, or the deviation of the losses might indicate an imperfection of the numerical model. It would be necessary to verify the results shown in Fig. 4 by measurements.

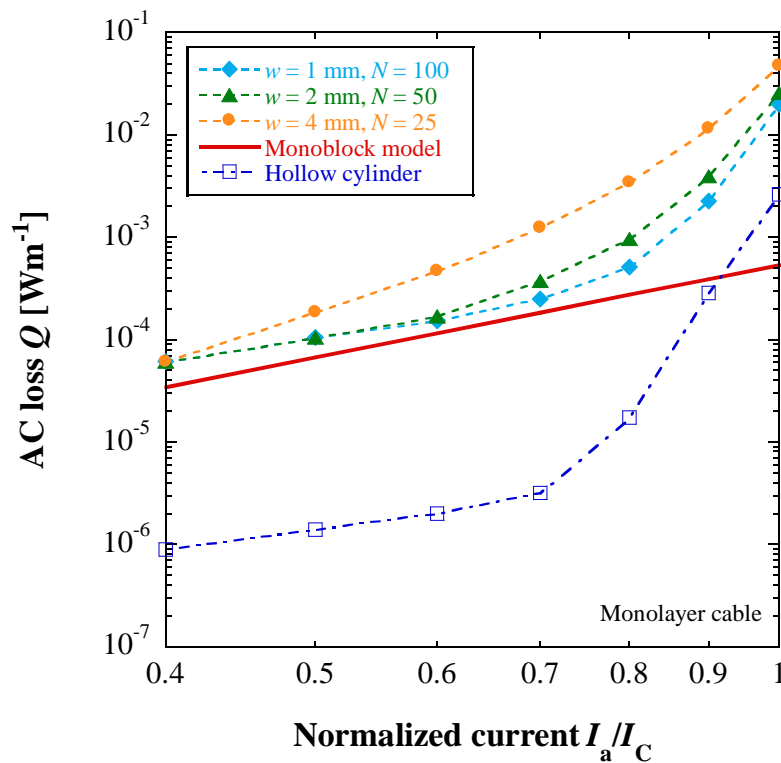


Fig. 4 AC losses in monolayer cable versus transport current (normalized by critical current) for various tape widths  $w$

### B. AC Loss in Double-Layer Cable

The losses in two-layer cables were also calculated by FEM. As in the monolayer cable, the loss calculation was first carried out by changing the tape numbers in both layers. Figures 5 (a) and (b) plot the relationship between the normalized AC losses in the first layer  $Q_1/N_1$  and the second layer  $Q_2/N_2$  of the two-layer cable and the normalized current  $I_a/I_C$  for various tape numbers  $N_1$  and  $N_2$ , where  $N_1 = N_2 = 4-25$ .  $Q_1$  and  $Q_2$  are the loss generated in the first layer and the second layer, and  $I_a$  and  $I_C$  denote the peak transport current and the critical current of the double-layer cable, respectively. The  $I_C$  of the double-layer

cable was obtained by multiplying the  $I_C$  of the tape (45.6 A) by  $(N_1 + N_2)$ . The layer currents  $I_1$  and  $I_2$  were assumed to be identical. Moreover, the relative tape-position angle between the layers, denoted  $\theta/\theta'$ , was assumed to be 0. Here,  $\theta'$  is the occupation angle of one tape in the second layer, calculated as  $2\pi/N_2$ . The  $\theta$  is the deviation angle between the perpendicular bisectors of the cross-section of REBCO tape in the first and second layers, as shown in Fig. 6. The relative angle  $\theta/\theta'$  quantifies the rotational dislocation between the first and second layers. The rotational dislocation is maximized at  $\theta/\theta' = 0.5$ , namely the tape on the gap (see Fig. 1 (b)). When  $\theta/\theta' = 1$ , the rotational dislocation is zero, namely the tape on the tape, and the cross-section of the cable becomes the same as the cross-section at  $\theta/\theta' = 0$ . In all calculations for the double-layer cable,  $N_1 = N_2$ . The cross-sections of the double-layer cables for  $\theta/\theta' = 0$  ( $N_1 = N_2 = 16$ ) are presented in Fig. 1 (a). The losses calculated by the thin-strip only outside of that layer and should not affect the loss in the first layer. However, on a microscopic scale, the second layer can generate vertical magnetic fields in the gaps between the tapes in the first layer. As can be seen in Fig. 1 (a), the gaps in both layers were assembled as  $\theta/\theta' = 0$ , meaning that the vertical fields were superimposed in the gaps; consequently, the losses were increased in the first layer. As  $N_1$  increased ( $N_1 \geq 24$ ), the loss in the first layer almost equalled the loss in the monolayer cable. When the gaps became sufficiently narrow, the vertical field generated by the second layer could not penetrate the first layer, so the losses in the first layer approximately equalled those in the monolayer cable. Next, how the normalized AC losses in the second layer ( $Q_2/N_2$ ) of the double-layer cable depended on the normalized current  $I_a/I_C$  were investigated by varying  $N_1$  and  $N_2$  as  $N_1 = N_2 = 4-25$ . For  $N_2 \geq 16$ , the normalized losses in the second layer almost matched those of the first layer. In that case, the gaps between the tapes in the second layer were sufficiently wide; consequently, the losses were dominated by the vertical magnetic fields at the edge of the tapes. Increasing the tape number to  $N_2 \geq 20$  reduced the vertical field, because the gaps were decreased.

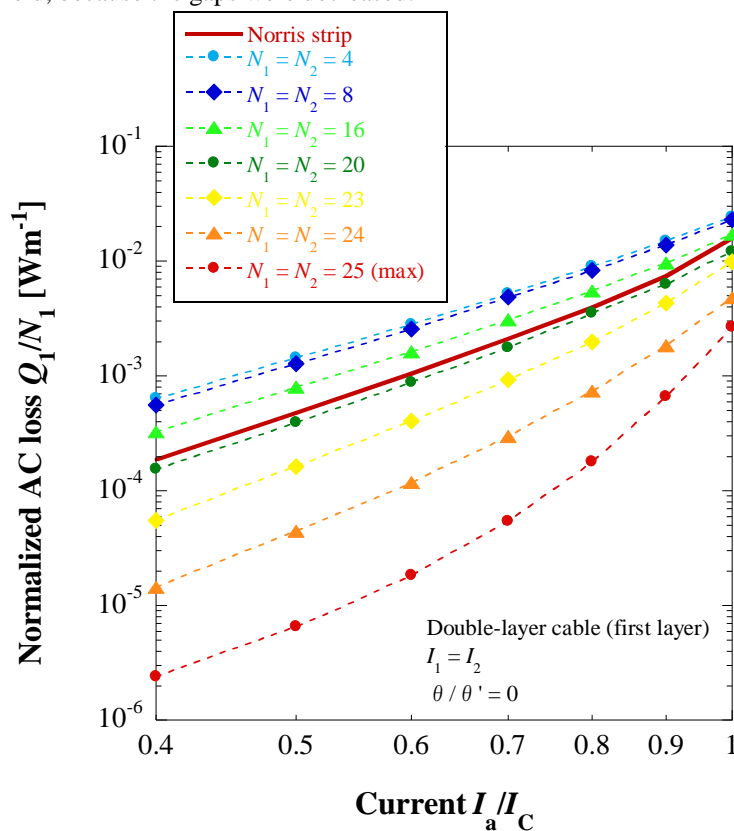


Fig. 5 (a) First-layer losses in double-layer cable versus transport current for various tape numbers  $N_1$  and  $N_2$

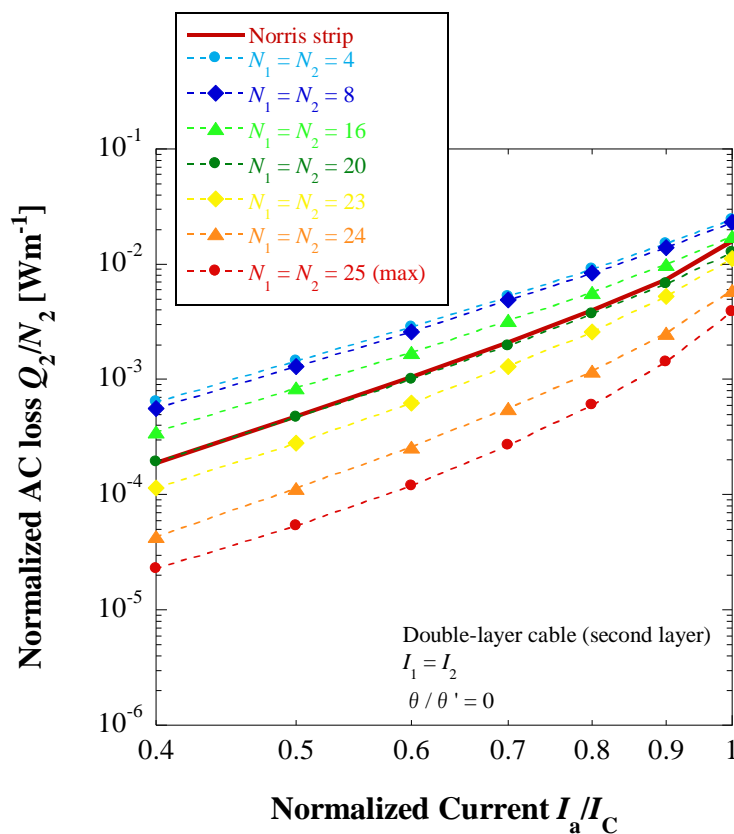


Fig. 5 (b) Second-layer losses in double-layer cable versus transport current for various tape numbers  $N_1$  and  $N_2$

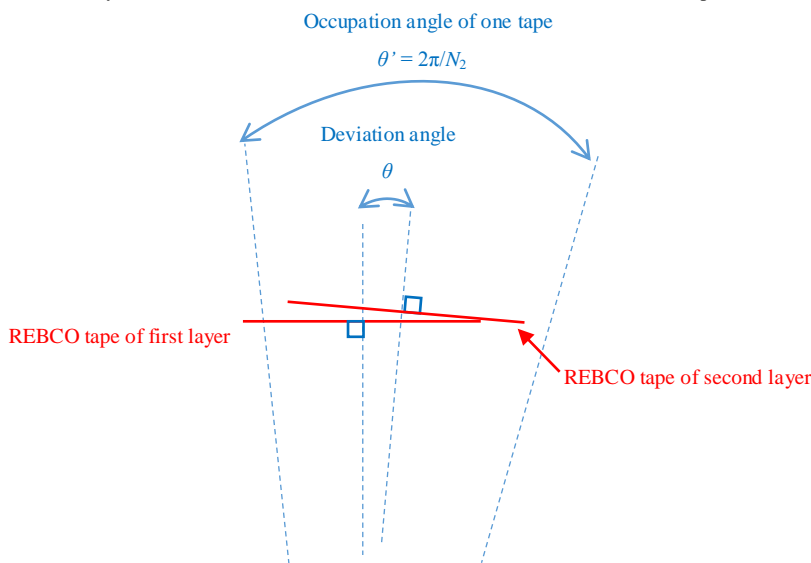


Fig. 6 Cross-section of two-layer cable with  $\theta/\theta' = 0.2$

From a macroscopic viewpoint, the tapes in the second layer experienced circumferential magnetic fields generated by the transport current passing through the tapes in the first layer. These circumferential fields increased the losses in the second layers with higher tape numbers. Therefore, the losses were higher in the second layer than in the first layer. Li, et al. reported that small gaps between the tapes are not absolutely essential to reduce the loss in multilayer cables [12]. The reduction of effectiveness by small gaps can be caused by the increase of the loss in the outer layer due to the circumferential fields.

The specifications of the double-layer cable described in Table 1 are those of Mukoyama’s cable [6], in which the tape number was  $N_1 = N_2 = 16$ . As mentioned above, the losses were calculated for  $\theta/\theta' = 0$ , but no information on the real value of  $\theta/\theta'$  exists in the report by Mukoyama. Thus, the  $\theta/\theta'$  of Mukoyama’s cable could be any value from 0 to 0.5. The value of  $\theta/\theta'$  would affect the loss in a double-layer cable with  $N_1 = N_2 = 16$ , because the gap is too wide to cancel the vertical field at the edge of the tape. Figure 7 plots the AC losses as functions of the angle  $\theta/\theta'$ , fixing  $N_1 = N_2 = 16$  and  $I_1 = I_2$  (yielding various normalized currents  $I_a/I_C$ ). Clearly, the losses depended on the angle and were minimized at  $\theta/\theta' = 0.5$ . When transport

current passed through the tape, the resultant self-field was strengthened at the edge of the tape, because the tape had a flat rectangular cross-section. This strengthened field was vertical to the tape face. Therefore, the author was interested in obtaining the magnetic field profiles around the tapes in the double-layer cable. Panels (a) and (b) of Fig. 8 plot the magnetic field profiles at  $\theta/\theta' = 0$  and  $\theta/\theta' = 0.5$ , respectively. In Fig. 8 (a), the same-side edges of the tapes in the first and second layers are completely aligned. Therefore, the vertical fields generated by the tapes in both layers have the same direction and are strengthened at the edges, increasing the loss in the cable. Conversely, when  $\theta/\theta' = 0.5$  (Fig. 8 (b)), the opposite-side edges of the tapes in the two layers are closed. At these edges, the vertical fields generated by the tapes in both layers are opposed and thus cancelled, reducing the loss in the cable. Therefore, to reduce the losses in double-layer cables constructed from 16 tapes in each layer, the relative angle between the layer orientations can be adjusted. However, this adjustment is effective only when the gaps between the tapes in both layers are comparatively wide. When  $N$  is large (e.g.,  $N_1 = N_2 = 25$ ), the loss is only marginally dependent on  $\theta/\theta'$ , because the vertical field between tapes in the same layer is automatically cancelled by the gap effect. In this case, the gap effect dominates any benefit gained by adjusting the angle.

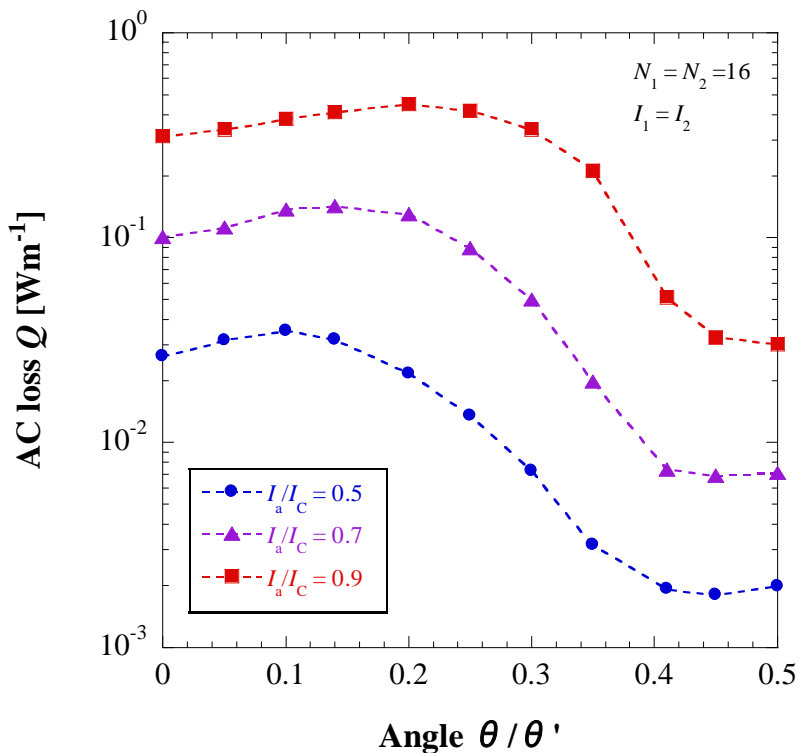
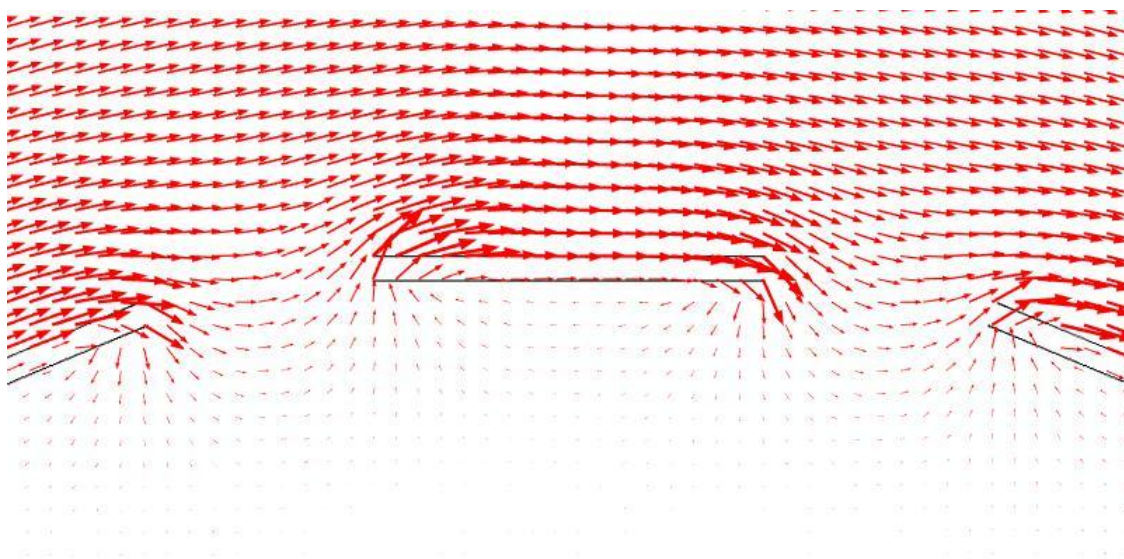
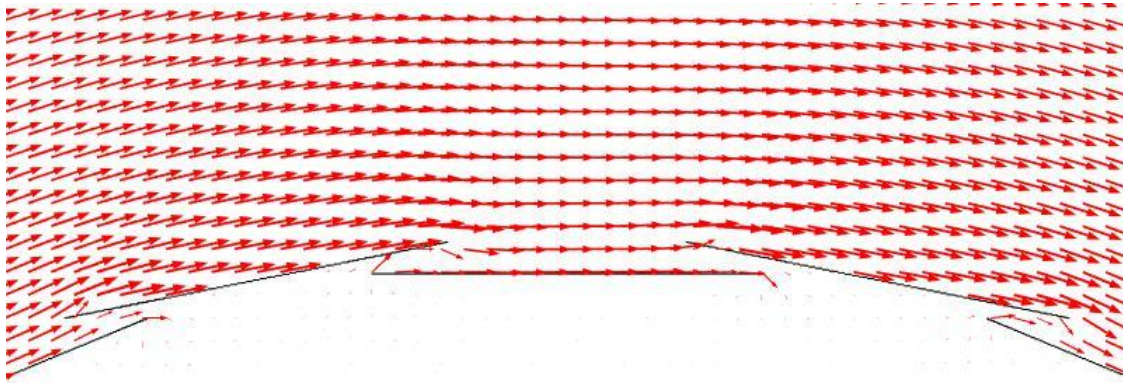


Fig. 7 AC losses in double-layer cable versus relative angle between tape positions of layers, determined at various transport currents (normalized by critical current)



(a)



(b)

Fig. 8 Magnetic field profiles around tapes in double-layer cable: (a)  $\theta/\theta' = 0$ ; and (b)  $\theta/\theta' = 0.5$ 

Finally, the calculated losses in the double-layer cable were compared to the measurements of Mukoyama, et al. [6]. Figure 9 plots the AC losses  $Q$  as functions of the normalized current  $I_a/I_C$  for various relative angles  $\theta/\theta'$ . The measured losses in Mukoyama's cable are indicated by solid red circles. As evident in Fig. 7, the losses drastically decreased at  $\theta/\theta' = 0.5$ . If all layers have the same helical pitch, the double-layer cable should be manufactured in this orientation to minimize the losses. However, the helical pitches differ among the layers in real cables, and the relative angle changes along the cable length; therefore, the losses vary along the cable length. To accurately determine the losses in real cables, a 3D FEM analysis may be required. Amemiya, et al. successfully accomplished 3D FEM analysis of the multilayer cable [14]. It would be beneficial to compare the results of quasi-3D FEM analysis (electric circuit model + 2D FEM) and 3D FEM analysis to understand the loss mechanism and to compare the computational superiority in the multilayer cables when the author has succeeded in developing both analyses. In the present calculation, which assumed  $I_1 = I_2$ , the losses in the first and second layers were almost identical at  $\theta/\theta' < 0.4$ . Therefore, equalizing the layer currents (i.e., setting  $I_1 = I_2$ ) minimizes the cable loss  $Q$ . The layer current can be adjusted by changing the helical pitch and the helical direction of the tapes in each layer. In Mukoyama's cable, the helical pitches (directions) in the first and second layers were fixed at  $P_1 = 340$  mm (S) and  $P_2 = 280$  mm (Z), respectively. Given these cable specifications and by applying the electric circuit model [11], the layer currents were computed to be  $I_1 = 301.3$  A and  $I_2 = 282.3$  A at  $I_a/I_C = 0.4$  ( $I_a = 583.6$  A),  $I_1 = 452.0$  A and  $I_2 = 423.5$  A at  $I_a/I_C = 0.6$  ( $I_a = 875.5$  A),  $I_1 = 602.7$  A and  $I_2 = 564.7$  A at  $I_a/I_C = 0.8$  ( $I_a = 1167.4$  A), and  $I_1 = 753.4$  A and  $I_2 = 705.8$  A at  $I_a/I_C = 1.0$  ( $I_a = 1459.2$  A). These equalities were attributed to the equal layer losses  $Q_1$  and  $Q_2$ , by which the cable loss  $Q (= Q_1 + Q_2)$  was minimized at  $\theta/\theta' < 0.4$ . However, when  $\theta/\theta' \geq 0.4$ , the second-layer loss  $Q_2$  slightly exceeded the first-layer loss  $Q_1$ . To minimize the loss at this relative angle, the second-layer current  $I_2$  might need to be set higher than the first-layer current  $I_1$ .

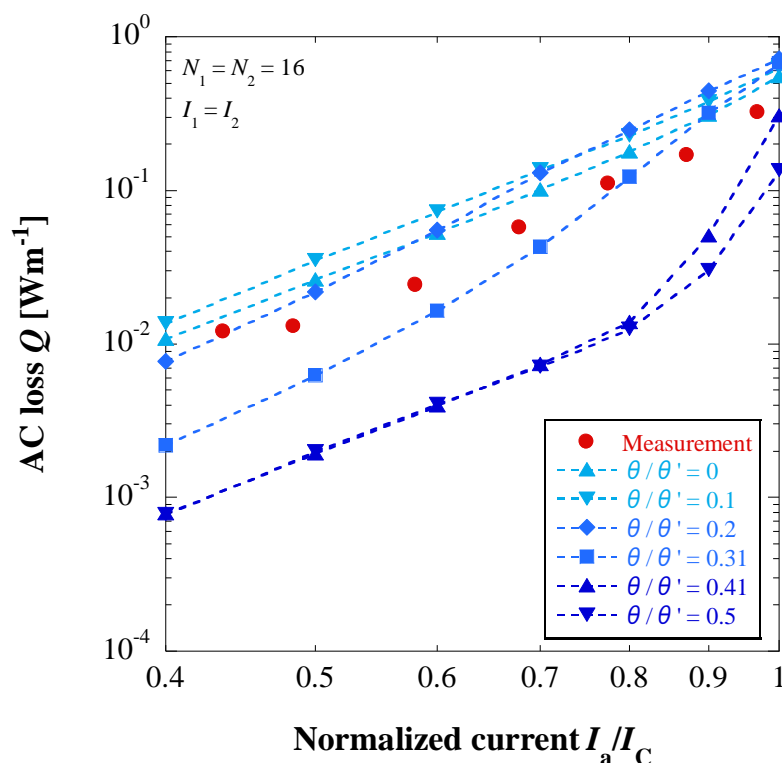


Fig. 9 AC losses in double-layer cable versus transport current, determined for various angles between tape positions in first and second layers

#### IV. CONCLUSIONS

This study evaluated current losses in REBCO cables using 2D FEM. To effectively reduce the loss in monolayer cables, the gap between the tapes were reduced by increasing  $N$ . This reductive effect was caused by the cancelation of the vertical magnetic fields applied to the gap. Alternatively, losses were reduced by decreasing  $w$ . In other words, the vertical field applied to the tape face was decreased by changing the cross-section of the cable from polygonal to cylindrical. In the double-layer cable, the losses in the first and second layers depended on the tape number; as the tape number increased, the losses became higher in the second layer than in the first. To reduce the total loss with high tape number, the first-layer current were set relatively higher than the second-layer current. Finally, when  $N$  was comparatively small, adjusting the relative tape-position angle between the two layers drastically reduced the loss. When  $\theta/\theta' = 0.5$ , the vertical fields at the tape edges in both layers cancelled each other, minimizing the loss in the cable. When  $N$  was large, the loss was dominated by the gap effect and was not reduced by altering the relative angle between the layers. In the 2D FEM calculations, the currents in both layers were assumed equal. However, in real cables, the tapes are helically wound onto the former; hence the layer current depends on the helical pitch and helical direction of each layer. To more accurately determine the cable losses, the 2D FEM should be combined with an electric circuit model, which computes the losses in helical cables. This undertaking will be attempted in future work.

#### REFERENCES

- [1] O. Maruyama, T. Ohkuma, T. Masuda, Y. Ashibe, S. Mukoyama, and M. Yagi et al., "Development of 66 kV and 275 kV Class REBCO HTS Power Cables," *IEEE Trans. Appl. Supercond.*, vol. 23, 5401405, 2013.
- [2] M. Konishi, Y. Shingai, T. Yamaguchi, and K. Ohmatsu, "Production of 6.5 km GdBCO conductors for 66 kV-5 kA class HTS model cable," *Physics Procedia.*, vol. 45, 141–144, 2013.
- [3] An He, Cun Xue, Huadong Yong, and Youhe Zhou, "Effect of soft ferromagnetic substrate on ac loss in 2G HTS power transmission cables consisting of coated conductors," *Supercond. Sci. Technol.*, vol. 27, 25004, 2014.
- [4] N. Amemiya, T. Tsukamoto, M. Nii, T. Komeda, T. Nakamura, and Z. Jiang, "Alternating current loss characteristics of a Roebel cable consisting of coated conductors and a three-dimensional structure," *Supercond. Sci. Technol.*, vol. 27, 35007, pp. 1–16, 2014.
- [5] Z. Y. Li, Y. H. Ma, K. Ryu, S. R. Oh, S. W. Yim, and S. D. Hwang, "Loss Test for a 5-m YBCO Cable Sample of the 22.9-kV KEPCO System Under Grid Operation," *IEEE Trans. Appl. Supercond.*, vol. 23, 5400704, 2013.
- [6] S. Mukoyama, M. Yagi, H. Hirano, Y. Yamada, T. Izumi, and Y. Shirohara, "Development of HTS power cable using YBCO coated conductor," *Physica C*, 445–448, pp. 1050–1053, 2006.
- [7] H. Noji, "Self-field losses in 1 m HTS conductor consisted of YBCO tapes," *Cryogenics*, vol. 47, pp. 343–347, 2007.
- [8] N. Amemiya, Q. Li, K. Ito, K. Takeuchi, T. Nakamura and T. Okuma, "AC loss reduction of multilayer superconducting power

- transmission cables by using narrow coated conductors,” *Supercond. Sci. Technol.*, vol. 24, 065013 (10pp), 2011.
- [9] N. Amemiya, Q. Li, K. Takeuchi, T. Nakamura, M. Yagi and S. Mukoyama et al., “Effects of lateral-tailoring of coated conductor for AC loss reduction of superconducting power transmission cables,” *IEEE Trans. Appl. Supercond.*, vol. 21, pp. 943-946, 2011.
- [10] H. Noji, S. Kawano, Y. Akaki and T. Hamada, “Calculating AC losses in high-temperature superconducting cables comprising coated conductors,” *Physics Procedia*, vol. 58, pp. 322-325, 2014.
- [11] A. P. Malozemoff, G. Snitchler, and Y. Mawatari, “Tape-Width Dependence of AC Losses in HTS Cables,” *IEEE Trans. Appl. Supercond.*, vol. 19, pp. 3115–3118, 2009.
- [12] Q. Li, N. Amemiya, K. Takeuchi, T. Nakamura, and N. Fujiwara, “AC loss characteristics of superconducting power transmission cables: gap effect and  $J_C$  distribution effect,” *Supercond. Sci. Technol.*, vol. 23, 115003, 2010.
- [13] G. Vellego and P. Metra, “An analysis of the transport losses measured on HTSC single-phase conductor prototypes,” *Supercond. Sci. Technol.*, vol. 8, pp. 476–483, 1995.
- [14] N. Amemiya, R. Nishino, K. Takeuchi, M. Nii, T. Nakamura, M. Yagi, and T. Okuma, “AC loss analysis of superconducting power transmission cables considering their three-dimensional geometries,” *Physica C*, vol. 484, pp. 148-152, 2013.